Abdominal Imaging



Abdom Imaging (2013)
DOI: 10.1007/s00261-013-0018-4

# TRUS–MRI image registration: a paradigm shift in the diagnosis of significant prostate cancer

F. Cornud,[1] L. Brolis,[2] N. Barry Delongchamps,[3] D. Portalez,[4] B. Malavaud,[5] R. Renard-Penna,[6] P. Mozer[7]

[1]Department of Radiology, Hôpital Cochin, Paris, France
[2]Koelis, Grenoble, France
[3]Department of Urology, Hôpital Cochin, Paris, France
[4]Department of Radiology, Hôpital de Rangueil, Toulouse, France
[5]Department of Urology, Hôpital de Rangueil, Toulouse, France
[6]Department of Radiology, Hôpital Pitié-Salpétrière, Paris, France
[7]Department of Urology, Hôpital Pitié-Salpétrière, Paris, France

## Abstract

Accuracy of multiparametric MRI has greatly improved the ability of localizing tumor foci of prostate cancer. This property can be used to perform a TRUS–MR image registration, new technological advance, which allows for an overlay of an MRI onto a TRUS image to target a prostate biopsy toward a suspicious area Three types of registration have been developed: cognitive-based, sensor-based, and organ-based registration. Cognitive registration consists of aiming a suspicious area during biopsy with the knowledge of the lesion location identified on multiparametric MRI. Sensor-based registration consists of tracking in real time the TRUS probe with a magnetic device, achieving a global positioning system which overlays in real-time prostate image on both modalities. Its main limitation is that it does not take into account prostate and patient motion during biopsy. Two systems (Artemis and Uronav) have been developed to partially circumvent this drawback. Organ-based registration (Koelis) does not aim to track the TRUS probe, but the prostate itself to compute in a 3D acquisition the TRUS prostate shape, allowing for a registration with the corresponding 3D MRI shape. This system is not limited by prostate/patient motion and allows for a deformation of the organ during registration. Pros and cons of each technique and the rationale for a targeted biopsy only policy are discussed.

**Key words:** Prostate cancer—Multiparametric MRI—TRUS-MRI image fusion

*Correspondence to:* F. Cornud; *email:* frcornud@imagerie-tourville.com

Published online: 17 July 2013

Taking a prostate biopsy decision is guided by the willingness to detect significant PCa in men with a reasonably long life expectancy and ideally harboring a still curable tumor. It is thus admitted world wide that biopsy and further staging investigations should be indicated only if they affect the management of the patient.

The current biopsy decision making, based on PSA level and/or DRE findings, has several drawbacks. Overdiagnosis of insignificant tumors, potentially leading to an unnecessary radical treatment, is now an established finding [1]. Under-diagnosis of aggressive tumor has also been well emphasized and fear for missing and/or underestimate tumor aggressiveness [2] often leads to repeat and saturation biopsies [3]. A substantial increase in biopsy-induced morbidity has been thus observed, mainly represented by prostatitis, especially in patients with no cancer and those with repeat biopsies [4].

Therefore, it becomes legitimate to identify men with potentially clinical significant PCa prior to biopsy and avoid detection of insignificant tumors by unnecessary biopsies. To achieve this goal, localisation of significant tumors by imaging is a pre-required step to allow for a targeted only biopsy strategy. Sensitivity of Trans Rectal Ultrasound (TRUS) is limited by the high number of isoechoic tumors originating in the peripheral zone (PZ) and its inability to detect transition zone (TZ) tumors due to the heterogenous pattern of benign prostatic hyperplasia (BPH). Specificity is limited by the high number of hypoechoic benign nodules. Accuracy of technological ultrasound (US) developments, such as microbubbles contrast injection [5], elastography [6], or computer-aided TRUS (histoscanning) [7] has not been validated yet, the main weakness of these techniques

being their limited ability to evaluate the anterior portion of the gland related to the high frequency of TRUS probes.

Conversely, MRI prostate magnetic resonance imaging (MRI) has undergone substantial technical improvements. In addition to morphological information provided by T2 weighted images, MRI allows for an estimation of physiological properties of tissues. Diffusion-weighted MRI (DWI) is sensitive to restriction of diffusion of water molecules [8], and dynamic contrast-enhanced (DCE) MRI can help estimate tumor angiogenesis [9]. As a result, multiparametric MRI has been shown to be efficient to localize and detect significant tumor foci within the prostate [10].

However, once a target has been identified on MRI, the physician performing the biopsy must have this information available at the time of biopsy to match as accurately as possible the needle tract and the target, hence the concept of TRUS–MRI image registration (or image fusion) to plan and to guide the biopsy. However, an accurate TRUS and MRI image registration requires to take into account prostate deformation and motion inherent to TRUS probe insertion and prostate scanning, which have strong implications in the accuracy of the registration process.

In this article, we review the different methods used for TRUS–MRI image registration and the published data which show how this technique can help to accurately detect significant prostate cancer.

## Methods of TRUS–MRI image registration

One method is cognitive and does not require any specific software. The other methods consist of co-registrating pre-acquired MRI data with real-time US with the use of software and computing of the probe location with a magnetic device placed on the probe [11] or incorporated in a robotic arm [12] defined as sensor-based registration. An other method consists of co-registrating TRUS and MRI images with an organ-based tracking system. A major difference exists between sensor-based and organ-based registration with regards to prostate deformation of MRI to TRUS images during registration as well as tracking prostate motion and deformation during biopsy. In this review, we describe and compare the accuracy of each technique.

## Cognitive registration

- MRI and TRUS images are superimposed by a cognitive overlay of TRUS and MR images during biopsy, using a printed document or by displaying MR images on the screen of a workstation located in the TRUS room, adjacent to the TRUS platform. Once the target is localized on MRI, the physician uses this knowledge to aim the biopsy needle at the prostate area where the previewed MRI shows a lesion (Fig. 1). Strictly speaking, the assimilation of visual overlay to software co-registration may be questioned. Cognitive overlay has been used during the last decade by default, since no alternative was available to use MRI findings for biopsy guidance. The extensive review by Moore et al. [13] summarizes results of cognitive registration obtained during this period. MRI protocol in most of these studies used either T2W-MRI alone or in combination with MRI-spectroscopy to perform targeted biopsies (TB). Overall results showed a trend for a higher performance of TB over random biopsies, in particular in case of anterior tumors [14]. In more recent studies, DCE and/or DW have become the most widespread standard of reference and been incorporated in the MRI protocol allowing for a more valuable evaluation of multiparametric MRI across studies, either before repeat or initial biopsy.
- Results of cognitive registration in protocols including DCE and/or DW-MRI. The six reported studies involved patients before initial biopsy.
  - Four studies support the value of cognitive registration to target biopsies.
    - Haffner et al. [15] (T2W + DCE-MRI protocol) compared, in a retrospective study, results of TB with those of 12 random biopsies in 555 patients. A TB only strategy would have necessitated only a mean of 3.8 cores per patient and avoid unnecessary biopsies in 38% of patients with a normal MRI, while avoiding the diagnosis of insignificant cancer detected by random biopsies in 13% cases. In this study, 13 significant cancers were missed with a targeted approach alone and 12 significant cancers were missed with a standard approach.
    - Labaranis et al. [16], in a series of 70 patients, showed that TB (T2W + DW + DCE-MRI protocol) allowed for an exact match of biopsy and surgical Gleason score in 90% cases and concluded that MRI should be performed before biopsy to solve the 35% underestimation rate of Gleason on random biopsies [17].
    - Park et al. (T2 + DW + DCE-MRI protocol) found a higher cancer detection rate (29.5%) in a group of 44 patients undergoing biopsy after MRI than in a group of 41 patients (9.8%) in a group of 41 patients submitted to random biopsies without MRI.
    - Puech et al. (T2 + DW + DCE-MRI protocol) found that MRI prior biopsy improved cancer detection rate which raised from 59% by sextant biopsies (SB) to 65% by TB under cognitive guidance. With regard to significant cancer (Ca length $>$ 3 mm on any core and Gleason

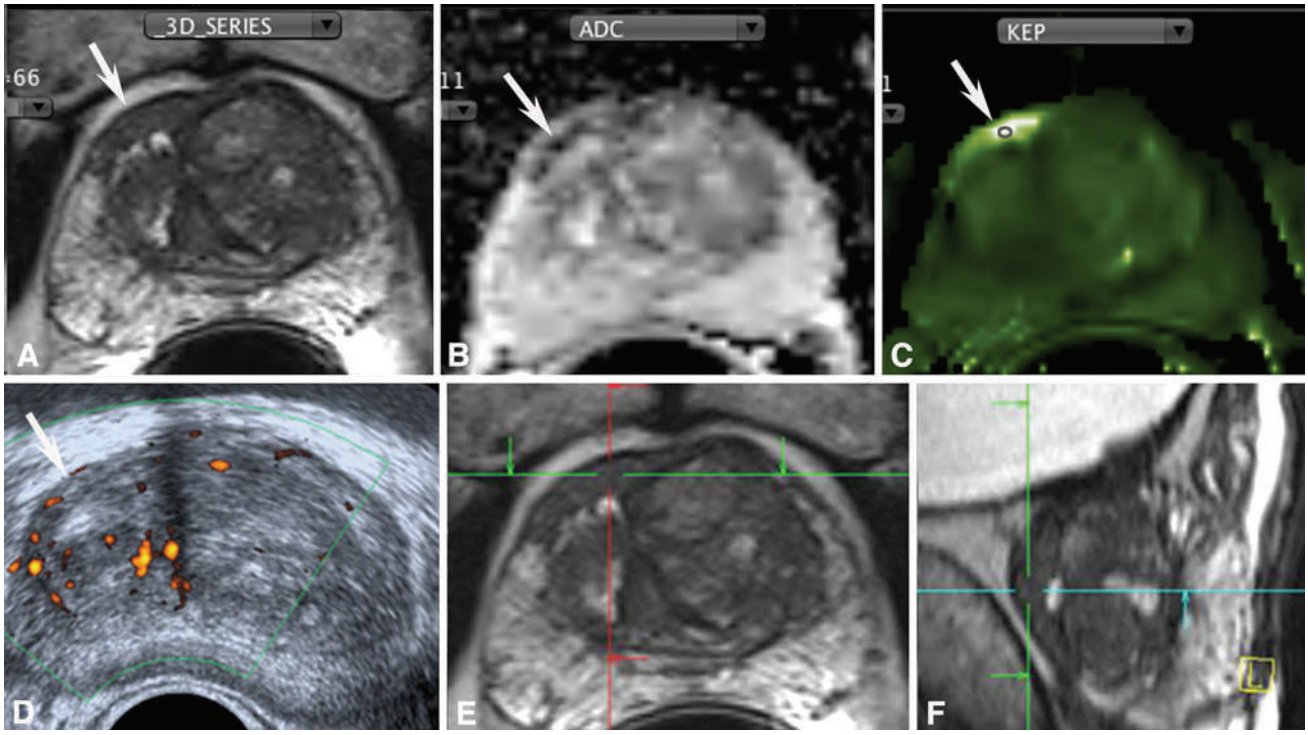


**Fig. 1.** Cognitive image registration. 65-year-old man. Three series of negative biopsies. Raising PSA level (11 ng/mL). **A–C** mp-MRI. Low signal intensity in the anterior part of the PZ with low ADC value and hypervascularisation (*arrow*). **D** The target is not visible on TRUS (*arrow*). **E**, **F** Cross referencing image, allowing for a cognitive image registration before biopsy. Three out of four positive TB, Gleason score 7, longest Ca length on one core: 8 mm.

grade > 6), cancer detection rate was 67% for TB and 52% for SB. Most of the 15 missed significant cancers were in the anterior regions of the prostate.

– Two other studies did not achieve a similar performance, in comparison to random biopsies.

  - Lattouf et al. [18], in a series of 26 patients (T2W and DCE-MRI protocol), did not find a significant difference in the detection rate between SB and TB and concluded that cognitive registration was insufficient to achieve an accurate overlay of MRI findings and TRUS images and that improvements in TRUS–MRI image registration was necessary to allow for a more accurate targeting.
  - Delonchamps et al. [19], in a series of 339 patients, prospectively evaluated the performance of SB vs three techniques of image registration TB and found that cancer detection rate with TB with cognitive image registration (42%) was not significantly higher than that of SB.

- Discrepancies across studies may be, at least in part, related to several factors like the absence of DW-MRI in the study by Lattouf et al. [18], or the absence of a precise knowledge of the location of the targets across studies. If only posterior lesions are considered, cognitive registration may not perform better than SB, whereas anterior lesions, whatever the zone of origin, may probably be better sampled by TB with cognitive registration in particular in large volume glands (>45–50 mL) [20]. It can thus be admitted that cognitive registration may add some value to SB. It can, however, be intuitively predicted that differences in slice orientation during acquisition between strictly axial MRI slices and the oblique scanning of end-fire TRUS probes (Fig. 2) explains why cognitive registration may fail to match with a sufficient accuracy the needle tract and the target. Moreover, the accuracy of cognitive registration also relies on the degree of expertise in prostate imaging. As a result, efforts have been deployed to develop image co-registration softwares to improve the accuracy of MRI-targeted TRUS-guided biopsies.

## Sensor-based registration

- This technique consists of a rigid geometric registration performed after paired landmarks have been

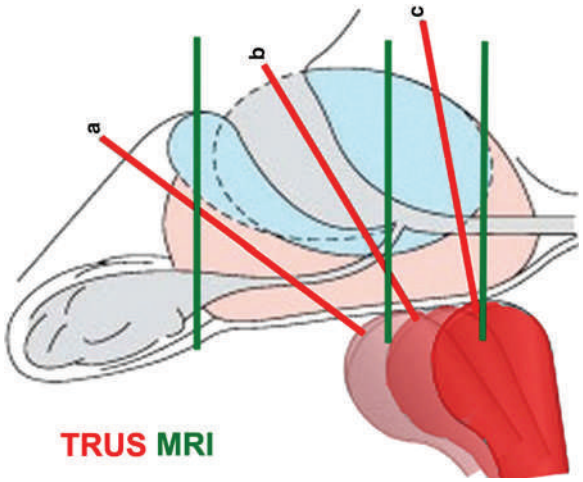


**Fig. 2.** Diagram showing differences in image acquisition during TRUS (*red lines*, oblique plane) and MRI (*green lines*, axial plane). This diagram shows how challenging can be cognitive registration to overlay an MRI focus with its corresponding location on TRUS.

selected on both TRUS and MRI (planning phase). State of the art rigid registration is done with a navigation device (sensor), magnetic in most cases. Once T2W-MRI datasets have been loaded into the US software, the spatial coordinates of the US probe are computed by the tracking device made of a transmitter placed close to the patient and a receiver placed on the TRUS probe (Fig. 3) .The planning phase of registration requires to define anatomical landmarks pairs between MRI and US by three points, one plane, or internal markers (Fig. 4), selected on MRI and then localized on TRUS during real-time prostate scanning. To optimize the registration, obliquity of the MR plane can be manually adjusted according to the assumed obliquity of the TRUS probe (Fig. 5). Once TRUS–MRI overlay is deemed acceptable, the navigation system is activated (guiding phase of the biopsy), allowing for a real-time TRUS scanning and MR-guided navigation. Biopsies are performed towards the registered image, assuming that no patient movement and no displacement or deformation of the prostate by the TRUS probe occur (Figs. 6, 7).

- Limitations of sensor-based registrations systems have been established. The prostate shape on TRUS and MRI is usually different, with or without the use of an endorectal coil. Images from MRI are thus simply superimposed onto US images and prostate contour is not deformed during registration [21]. Mismatches can occur during attempts to match both prostate contours and internal landmarks (Figs. 4, 5). Moreover, sensor-based systems only track the TRUS probe and not the prostate itself. They thus do not allow for an organ-based registration as they do not take into account the anterior displacement of the gland which occurs during TRUS scanning, leading to a loss of overlay between TRUS and MRI registrated images [21]. Registration has thus to be repeated and is subjected to the same caveats as those encountered during the initial registration, and errors in targeting can occur. As a result, the topographic precision of this type of rigid registration may not exceed 5–10 mm [22].
- Clinical results of sensor-based registration. The accepted limitations of sensor-based image registration probably explain why accuracy of this system varies across studies when it is compared to SB and cognitive registration TB.
  - In the comparative study by Delongchamps et al. [19] (initial biopsy) of different image registration techniques, rigid registration-based TB (ESAOTE navigation system) cancer detection rate of significant cancers was significantly higher than that of SB and cognitive registration TB.
  - Mouraviev et al. [23] in a small series of 32 consecutive patients with a raising PSA level and a setting of repeat biopsy found a 46% cancer detection rate with rigid registration TB (ESAOTE navigation system, Italy), significantly higher than that of cognitive registration (33%).
  - Puech et al. [20] found that sensor-based registration TB, although performing better than SB, did not provide a higher accuracy than that cognitive registration TB (ESAOTE navigation system, Italy).

### *Sensor-based registration with computer-aided planning phase*

To improve the accuracy of sensor-based registration, two systems have incorporated a software to increase the accuracy of the planning phase of rigid registration.

- The first is the Artemis system [24].
  - In this system, the TRUS probe is attached to a robotic arm and sensors are incorporated in the joints of the arm. During the planning phase, the prostate is scanned in a 2D mode. Images are captured by the Artemis device and assembled into a 3D volume displayed on screen [12]. TRUS prostate segmentation is then performed and the prostate is then digitally reconstructed on screen in real time. MRI segmentation and placement of a ROI on the target are done prior to biopsy. During the guiding phase, MRI data are loaded in the Artemis device and registration begins by manual selection of pair landmarks (base, apex…). Once TRUS and MR images are aligned, a surface-based registration algorithm, requiring a prostate segmentation, is used to match MRI and

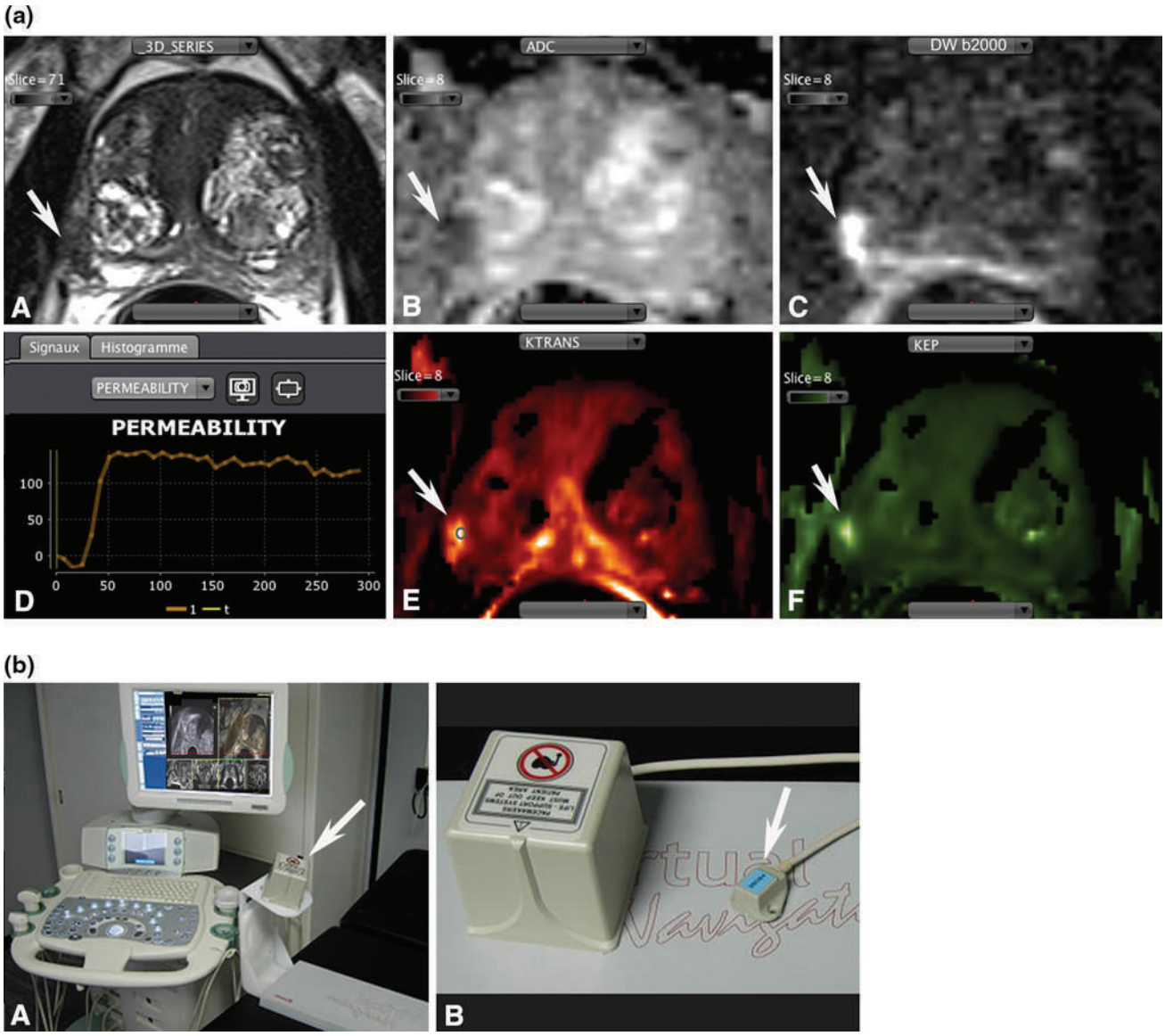


**Fig. 3.** Sensor-based image registration. 67-year-old man. Raising PSA (7 ng/mL). **a** mp-MRI: low signal intensity focus in the right PZ (*arrow*, **A**), with low ADC value and high intensity signal on source DW images at high *b*-value (*arrow* **B**, **C**) and increased vascularization (*arrow* **D–F**). **b** Sensor-based navigation system with a magnetic device including a receiver placed close to the patient (*arrow* **A**) and a receiver placed on the TRUS probe (*arrow* **B**).

TRUS prostate contour, requiring total patient immobility to achieve a reliable registration. The biopsy is then performed like with navigation systems. In the study by Natarajan et al. [12], the precision of the device is reported to be $1.2 \pm 1.1$ mm, provided that total immobility of the patient can be maintained.

– Clinical results have been reported in two studies by the group which performed a clinical evaluation of the original model developed by Bax et al. [24]. The first study [25] included 171 men who underwent a repeat biopsy in a setting of active surveillance or of a negative first set of biopsies. Ca detection rate was significantly higher (21%) in TB than in SB (7%). Of the 40% of men with Gleason score 7 Ca, 40% of them were detected by TB only. The second study [26] involves 105 men with a previous set of negative biopsies. Ca detection rate by TB was 34%. Of them, 72% were significant tumors. In both studies, the degree of suspicion on MRI was the most powerful predictor of significant cancer on multivariate analysis, as cancer detection rate was 86%–95% in patients with a highly suspicious MRI target (score 5).

- The second device is the Uronav system developed by Philips (Philips Medical Systems, Bothell, WA, USA)

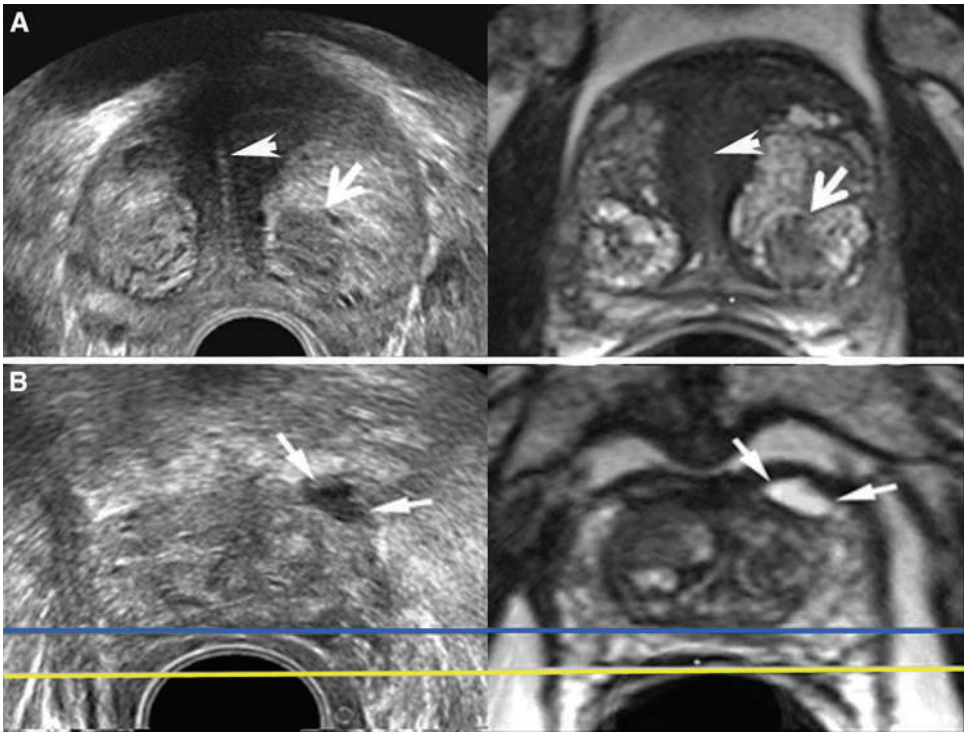


**Fig. 4.** Planning phase of sensor-based registration: Paired landmarks are selected on both imaging modalities. **A** Left BPH nodule (*arrow*) and prostatic urethra (*arrowhead*) are aligned on both modalities. **B** Glandular dilatation of the anterior part of the left apex (*arrow*) is aligned on both modalities. However, the posterior aspect of the prostate on TRUS (*blue line*) is not aligned on MRI (*yellow line*).

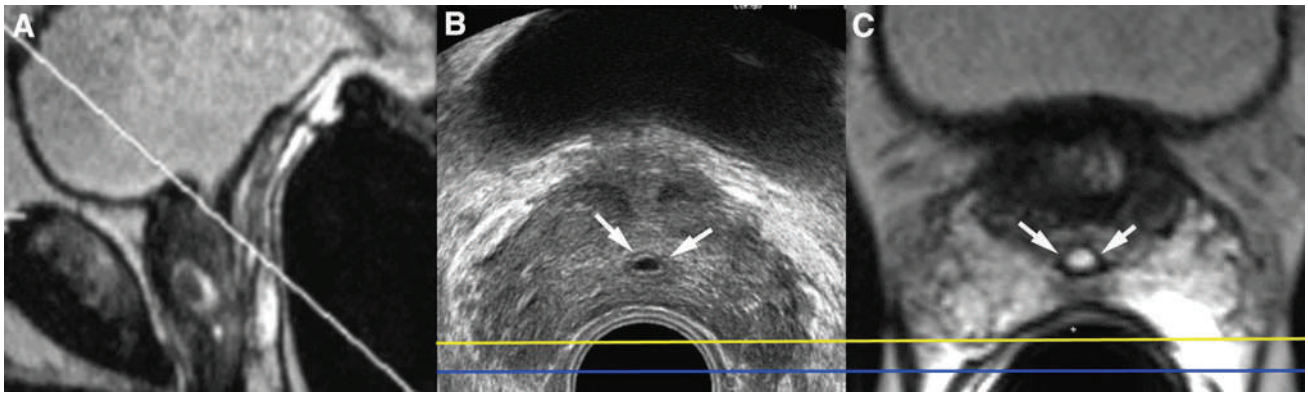


**Fig. 5.** Planning phase of sensor-based registration. The prostate volume has been oriented in an oblique plane (**A**) to allow for a registration of the utricule (*arrows* **B**, **C**), but the posterior aspect of the prostate on TRUS (*blue line*) is not aligned on MRI (*yellow line*).

in which spatial tracking of the TRUS probe is done by sensors embedded in a needle guide.

– During the planning phase, a 2D-TRUS acquisition is performed and, similarly to the Artemis system, images are reconstructed into a 3D volume. Registration of the 3D TRUS volume with MRI is done manually by in house software [27] at an adjacent workstation by displaying on screen the three orthogonal views of the 3D-TRUS and MRI together with the MRI segmentation. Manual mapping of the 3D-TRUS onto the MRI achieves the equivalent of non-rigid registration but at the expense of substantial interaction during the procedure to align both internal landmarks and prostate surface. During the guiding phase, the biopsy is performed under real-time guidance, like with the ESAOTE system. A software is incorporated in the system which allows for small motion correction of the prostate [28]. The targeting error of the system has been evaluated on a phantom model and estimated to 2.4 ± 1.2 mm [28].
– Clinical results of the Uronav platform have been reported by the group which participated to the development of the system.
  - In a first study, Pinto et al. [29] reported the cancer detection rate of sensor-based registra-

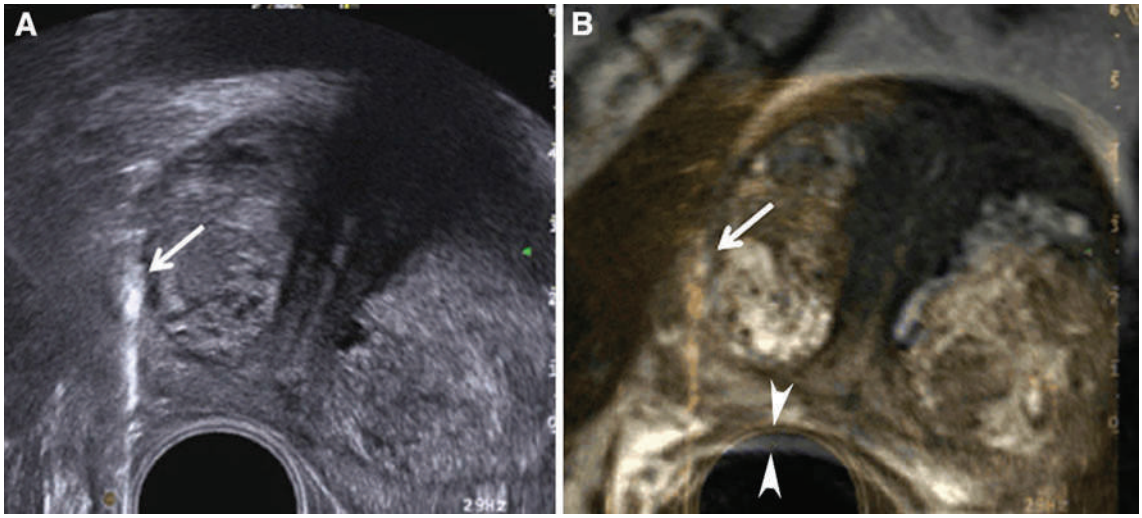


**Fig. 6.** Sensor-based registration. Guiding phase of the biopsy. Same patient as Fig. 3a. The needle tract (*arrow*), visible on TRUS (**A**) can be seen on the overlayed MR image (**B**). In this example, despite the prostate tilting during biopsy, the posterior aspect of the prostate remains aligned on both modalities (*arrowheads*).

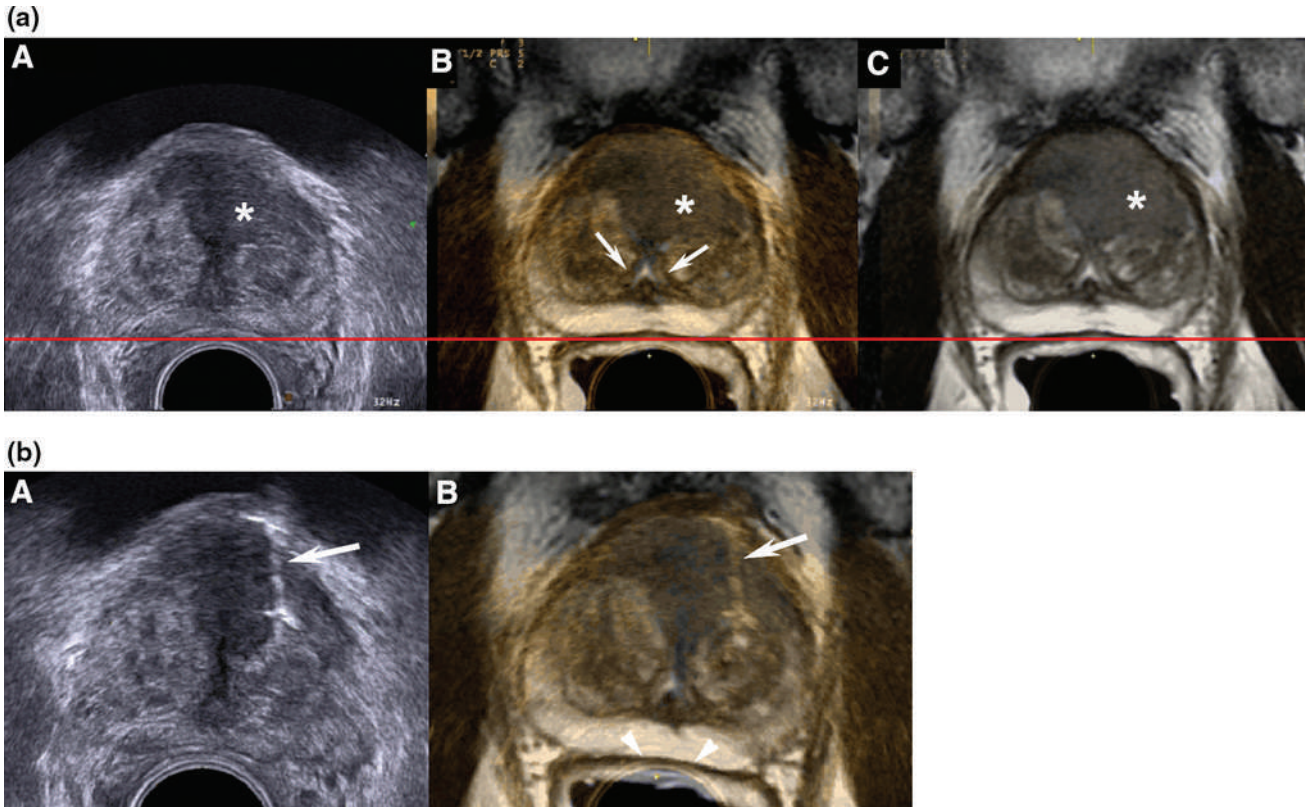


**Fig. 7.** Sensor-based registration. 66-Year-old patient with an elevated PSA level (12 ng/mL). No previous biopsy. **a** planning phase of the biopsy (**A**–**C**). The pair landmark for registration is the veru-montanum, well visible on both modalities (*arrow*). Suspicious area on MRI in the anterior part of the TZ (*), retrospectively detectable on TRUS. The posterior aspect of the prostate is aligned (*red line*) **b**: guiding phase of the biopsy. The needle tract (*arrow*), visible on TRUS (**A**) can be seen on the overlayed MR image (**B**). In this example, the posterior aspect of the prostate remains aligned on both modalities (*arrowheads*) during biopsy.

tion in 101 patients including patients with no prior biopsy, with a prior negative biopsy and with a prior positive biopsy (approximately one-third in each group). Cancer detection rate by TB was calculated according to the level of suspicion of cancer on mp-MRI: it was 28; 67%

and 89%, in low, moderate, and high suspicion, respectively. Overall, cancer detection rate was twice that of SB.

- In a second study, Vourganti et al. [11] in a setting of repeat biopsy found a 37% cancer detection rate of combined SB and rigid registration TB. High grade cancer was undetected by random biopsies in 55% of cases. TB allowed for a pathological upgrading in almost 40% cases. The authors concluded that multiparametric magnetic resonance imaging with a magnetic resonance imaging/US fusion biopsy platform was an ideally suited diagnostic tool for detecting prostate cancer in patients with negative transrectal US biopsies presenting with a persistent biological/clinical suspicion for cancer.

## *Sensor-based registration: conclusion*

Sensor-based image registration may improve the accuracy of random biopsies, probably to detect anterior tumors, but may not be superior to cognitive registration. Its main advantages are to be a real-time technique and embarked in several commercially available US platforms. They may thus represent an appealing technique for physicians involved in TRUS-guided prostate biopsies. Nevertheless, sensor-based registration with navigation systems does not represent an organ-tracking technique, the sensors only allowing for a TRUS probe-tracking which does not take into account patient and/or prostate motion during the procedure. Improvements incorporated in the Artemis or the Uronav systems have been developed to circumvent this major limitation, but accuracy may still be limited if patient and organ immobility, critical in sensor-based registration, is not consistently obtained. Moreover, a prostate deformation cannot be obtained related to the fact that the probe only performs an initial 3D acquisition during biopsy and the 2D scanning during the tracking phase cannot be registered in real time to the reference volume. This other limitation explains why researchers have developed mathematical models and softwares to provide tools to perform a more consistent image registration accuracy.

## *Organ-based registration*

The principle differs from that of sensor-based registration [22], because the computer tracks the organ itself, not the TRUS probe. The planning phase of this technique combines three steps in the registration process to obtain the final overlay of 3D-TRUS (reference volume) and MRI volumes. Two rigid registrations are first performed to superimpose the 3D shapes, representing the organ contour on both images. Then, an algorithm is used to deform the MRI shape to match the TRUS shape to obtain the final 3D deformable registration (Fig. 8). The final guiding phase is an automatic TRUS–TRUS voxel-based registration to accurately track the target [22].

- *The planning phase of organ-based registration* requires a 3D acquisition of the prostate volume which is performed with a motorized TRUS probe. Acquisition is automatic and does not require to swap the prostate to assemble 2D images in a 3D volume, thus avoiding organ displacement. The 3D-TRUS prostate volume is displayed on screen.
  - *The first step is a rigid landmark-based registration*, comparable to that performed during sensor-based registration. It is obtained by the placement of three anatomical landmarks on both imaging modalities (Fig. 9). Similarly to sensor-based registration, this approach is sensitive to landmark identification errors and paired landmarks have to be placed at the same anatomical location on both images.
  - *The second step is a multiple point-based rigid registration*, which is not performed in pure sensor-based registration. It utilizes a shape-statistics-based semi-automatic prostate surface delineation (surface-based registration) [30]. Statistics-driven semi-automatic segmentation yields more reproducible results than those of landmark-based registration with less surface variability, which improves the final accuracy of the registration. The segmentation uses shape assumptions and properties to predict the 3D surface of the prostate. The delineation process deforms the statistical shape (composed of 3000 points), which interpolates the ten to twenty points previously selected by the operator. This approach allows for a fast segmentation and avoids the discontinuities commonly observed in multislice segmentation. With this technique, the multiple point-based rigid registration is finally done with 3000 surface points defining the 3D shape (prostate mesh) on each imaging modality, which substantially increases the accuracy of rigid overlay of both the shapes and the reproducibility of the segmentation process.
  - *The third step consists of an elastic 3D organ-based registration*. The multiple point-based technique keeps the same limitations than sensor-based registration. It does not compensate for the deformation of the posterior aspect of the prostate induced by rectal probe insertion and does not take into account prostate displacement during TRUS scanning. To circumvent these limitations, deformation of the organ is necessary to minimize the distance between each of the multiple points (prostate mesh) defining the TRUS and the MRI shapes. An algorithm achieves 3D elastic deformations that further minimize the distances between each point of the MRI and the TRUS shapes. The deformable registration is

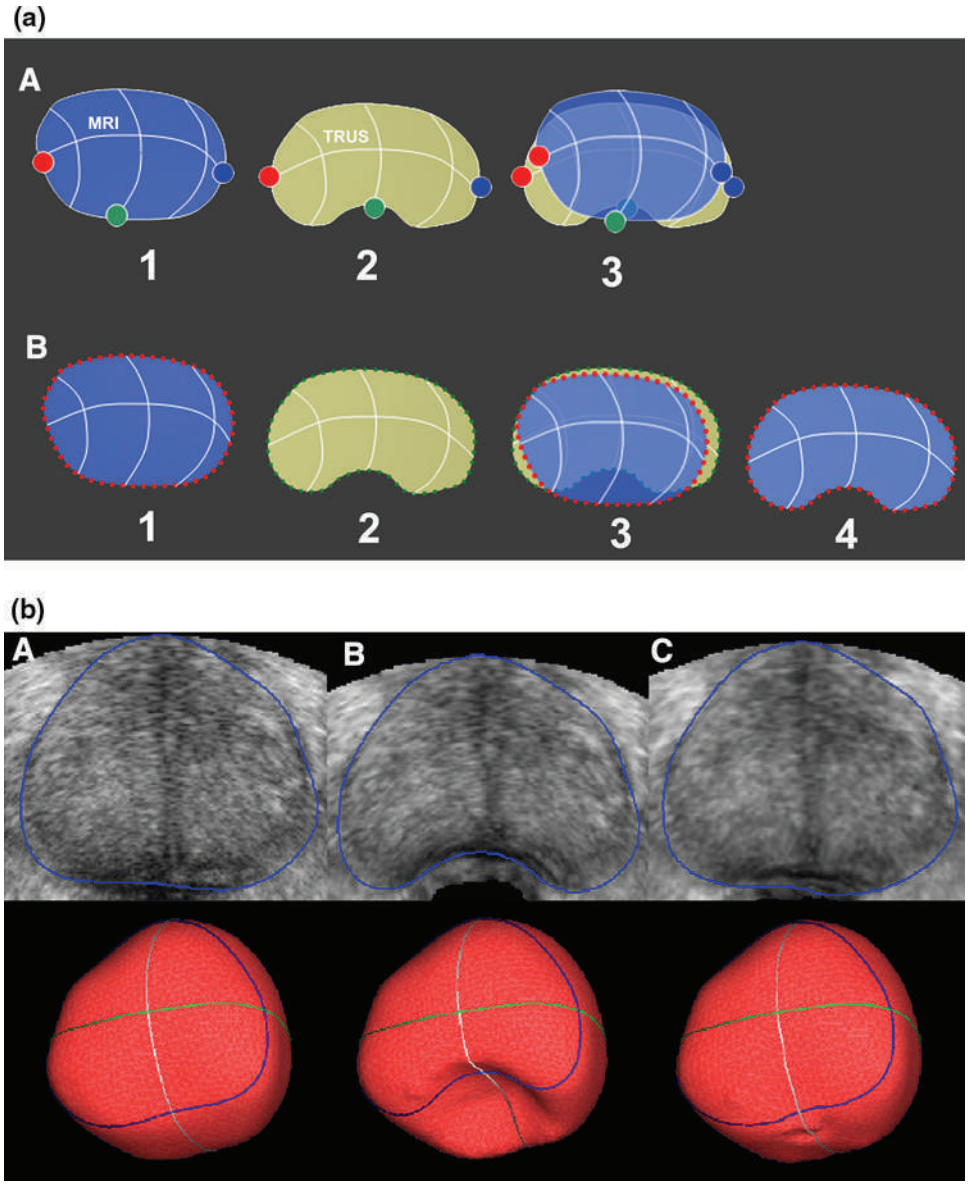


**Fig. 8.** Diagram explaining differences between rigid (non deformable) and elastic (deformable) registration. **a** Rigid registration. **A** Three points have been placed on the MRI (1) and on TRUS prostate contour (2). Differences in prostate shape and deformation do not allow for an accurate prostate overlay after rigid registration (3). **B** Elastic deformation with surface-based registration and organ deformation. Multiple points have been placed on MRI and TRUS prostate contour (1, 2). This first step is a rigid registration which still lacks accuracy owing to the differences in prostate shape (3). An algorithm allows for a deformation of the MRI prostate shape to allow for an accurate registration (4). **b** Demonstration of the efficiency of elastic deformation. **A** The original shape of the prostate with its correspondent 3D shape (*red image*, *lower row*). **B** Induction with a mathematical model of a posterior deformation of the prostate (10-mm-diameter sphere to simulate TRUS probe insertion). **C** After activation of the elastic registration software, the original 3D shape has been rebuilt.

applied both at the surface and in the inner volume of the shape and its corresponding structures.

– *The accuracy of the planning phase of organ-based registration* has been evaluated on 49 patients (Brolis et al., unpublished data). One hundred and twelve TRUS and MRI landmarks were selected. The first rigid step provided a mismatch of 3.6 ± 2.2 mm. After the second rigid step with multiple point registration, the mismatch fell to 2.1 ± 1.0 and to 1.7 ± 0.7 mm after elastic registration. The most important failures are represented by the 10% highest mismatches which showed a mean difference of registration of 7.7 ± 2.8 mm after the first rigid registration, falling to 4.6 ± 1.6 mm after surface-based registration and to 3.5 ± 1.7 mm after elastic registration. The worst case with an initial error of

15.1 mm after the first rigid registration decreased to 3.3 mm after surface-based registration, and finally to 2.6 mm after elastic registration, which divided the initial error by five. Ukimura et al. [31] validated the accuracy of the technique on a phantom model containing low signal intensity lesions. Of the 27 biopsies done with elastic registration, 89% of them hit the lesion and the targeting error was estimated to 2.09 ± 1.28 mm (0 mm in 28% of cases, 1–2 mm in 39% of cases, 2–3 mm in 9% of cases and ≥3 mm in 24% of cases).

- *The guiding phase of the biopsy*. Once the target has been delineated on the MRI image registered with the reference TRUS image, a 3D-TRUS acquisition is performed with the probe aiming the assumed location of the target. This is followed by a TRUS–TRUS monomodal image registration between the reference TRUS image, previously obtained during TRUS–MRI registration, and the 3D-TRUS volume acquired just before biopsy.
  - This registration process requires three steps (Fig. 10), the first two consisting of a rigid registration. The final step is an elastic registration. However, the principles of monomodal TRUS–TRUS registration are entirely different from those of geometric TRUS–MRI registration. It is a voxel-based (iconic) tracking allowing for an automatic registration of 3D-TRUS volumes. The algorithm allows for a spatial transformation of one of the volume until similarities with the other volume can be obtained allowing for an overlay of the two volumes. The first rigid registration uses a model which computes the plausible position of the prostate on the acquired volume which is then registered with the reference volume. This first estimate (Fig. 10A) is followed by a more general rigid registration model with six degrees of freedom which refine the initial estimation (Fig. 10B). These two computations are done on the entire TRUS volume overlay. In the final step of the registration (Fig. 10C), an elasticity constraint is applied to obtain thousands of local displacements in the neighborhood of each voxel. The final result is an accurate overlay of the acquired and the references volumes. The required computational time does not allow for a real-time registration, and it takes 4 s after each acquisition, i.e., after each biopsy, for the registered images to be displayed on screen.
  - The accuracy of automatic monomodal 3D-TRUS fusion has been evaluated [22] on 40 patients and 687 fiducials placed in the center of small structures (calcifications, cysts). The two rigid steps achieve a tenfold decrease of the targeting error. The obtained 1.4 ± 0.8 mm accuracy is still increased after elastic deformation yielding 0.8 ± 0.5 mm. In the 10% worst cases with a mean initial error of 17.9 mm, the process reduces the mean distance to 2.0 mm (89%).

**Fig. 9.** Elastic registration. 69-year-old man with an elevated PSA level (9 ng/mL). No previous biopsy. **a** mp-MRI. Low signal intensity lesion in the anterior part of the TZ (*arrows*, **A**) with hypervascularisation (*arrows*, **B**), low ADC value (*arrows*, **C**) and high intensity signal on DW-MRI at high *b*-value (*arrows*, **D**). **b** Rigid registration including the first two steps of the process. A pre-acquired 3D volume is displayed on screen (**A**–**C**). Ten to twenty points have been placed (second step) on the prostate contour (**A**) which refine the first step of the registration performed by placement of three landmark points at the apex, base, and posterior surface of the prostate (*colored points*, **B**). The result of the multiple points registration is displayed in **D** showing the prostate mesh, corresponding to the 3000 points used for the rigid registration. **c** The same procedure has been applied on the 3D-TRUS acquired volume (**A**–**C**). The prostate mesh is well visible (**D**). **d** Placement of a ROI on the target (*yellow circle*), visible on the axial and sagittal planes of T2W (**A**, **B**) and DW-MRI (**C**, **D**). **e** The TRUS–MRI elastic fusion has been performed. The target (*yellow tag*) is visible on both modalities (**A**). A first biopsy is performed aiming at the abnormal area (*arrows*, **B**). After TRUS–TRUS fusion, the needle tract (*green tag*) is displayed within the target (**C**). **f** Three biopsies are performed, all traversing the target (**A**–**C**). Gleason score 7 (4 + 3), confirmed at pathological examination of the specimen, showing a TZ anterior tumor (*arrows*, **D**).

- Performing the biopsy.
  - If the target is visible on TRUS, the biopty gun is activated and a TRUS 3D acquisition is performed, needle left in place. After TRUS–TRUS image registration, the displayed registrated image shows if the needle track has run into the target. This can be indifferently checked on the TRUS or MRI image (Fig. 9f).
  - If the target is not visible on TRUS, a virtual biopsy is performed by aiming the presumed TRUS location of the target without activating the biopty gun to ensure that the virtual track is through the target (Fig. 11). An adjustment may be necessary and the virtual biopsy is repeated until matching of the needle tract and the target is obtained. Then, one to three cores are taken from the target. To limit the number of cores to two or three, a virtual biopsy is recommended before each real biopsy, in particular in small size foci (<1 cm).
- *Clinical results of TRUS–MRI organ-based registration*. Currently, only few studies are available, related to the ongoing validation of the accuracy of the system.
  - Portalez et al. [32], in a clinical setting of repeat biopsies, showed that the overall positive biopsy

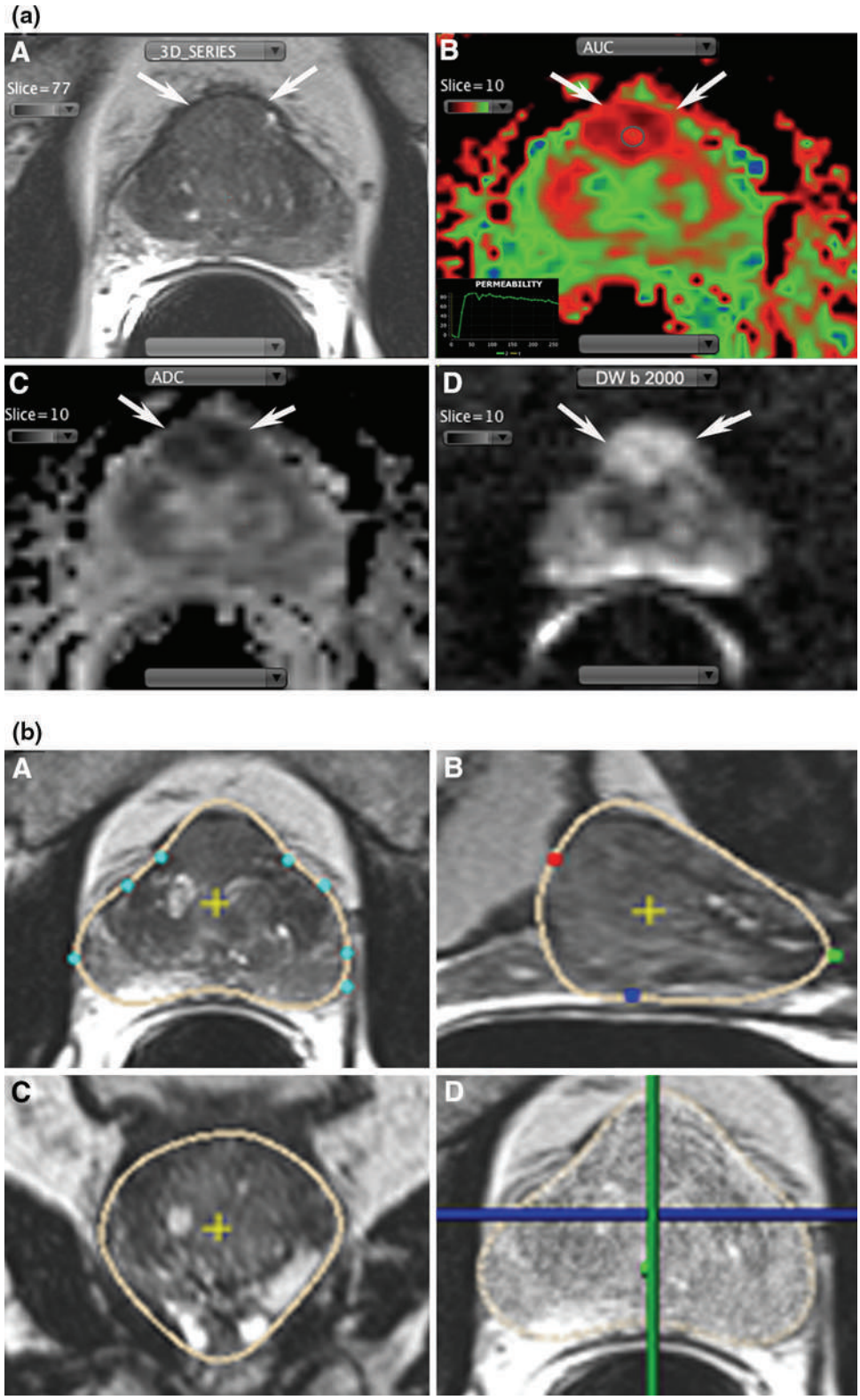


rate of TB was 36.3% vs 4.9% in SB only performed in sextants without MRI target. With the use of the ESUR guidelines [41] and the five-point scale Likert score, the positive biopsy rate ranged from 3% (score 1) to 83% (score 5). TB provided a significant longer Ca length than SB, but no difference in Gleason score was observed in this study.

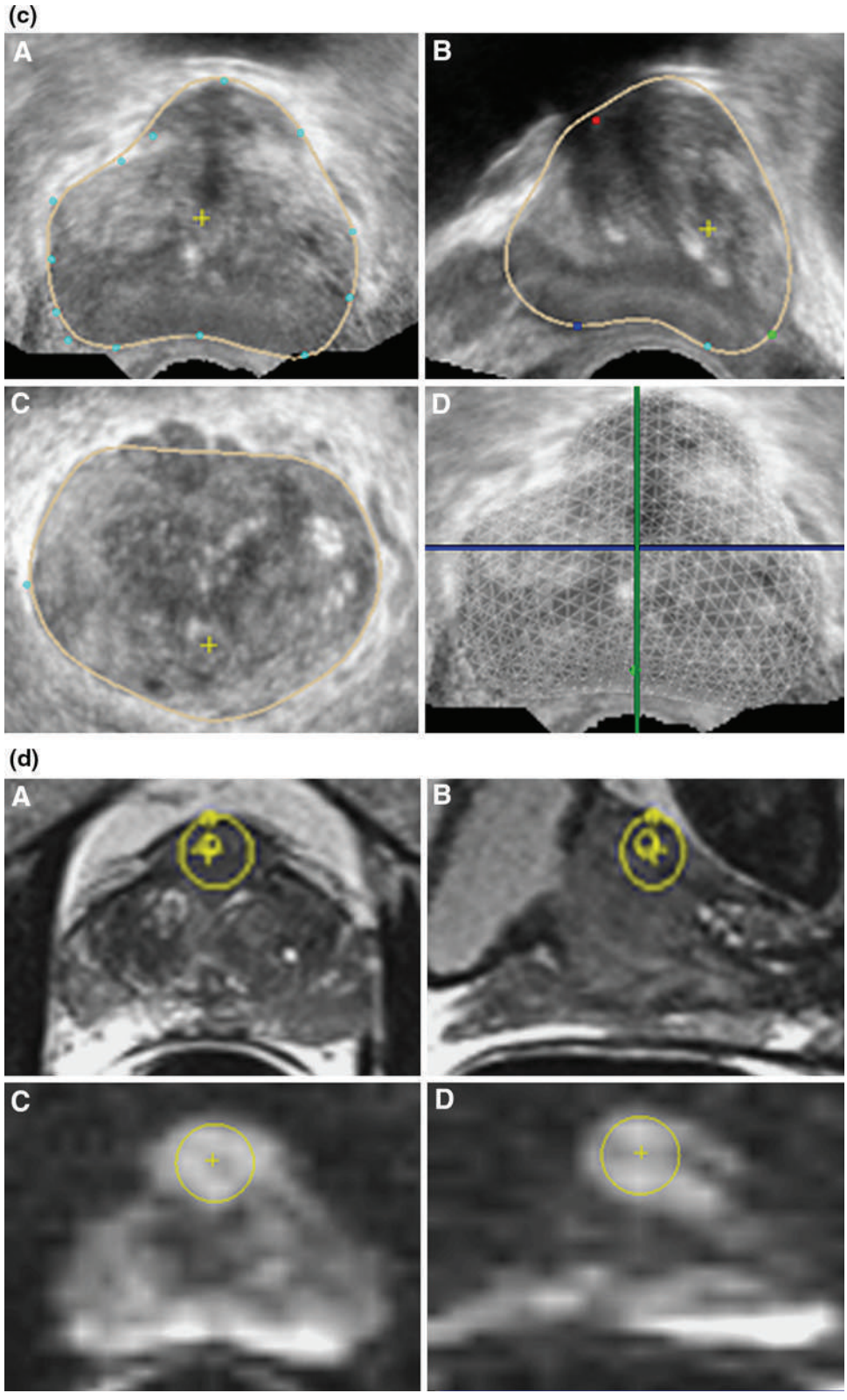


**Fig. 9.** continued

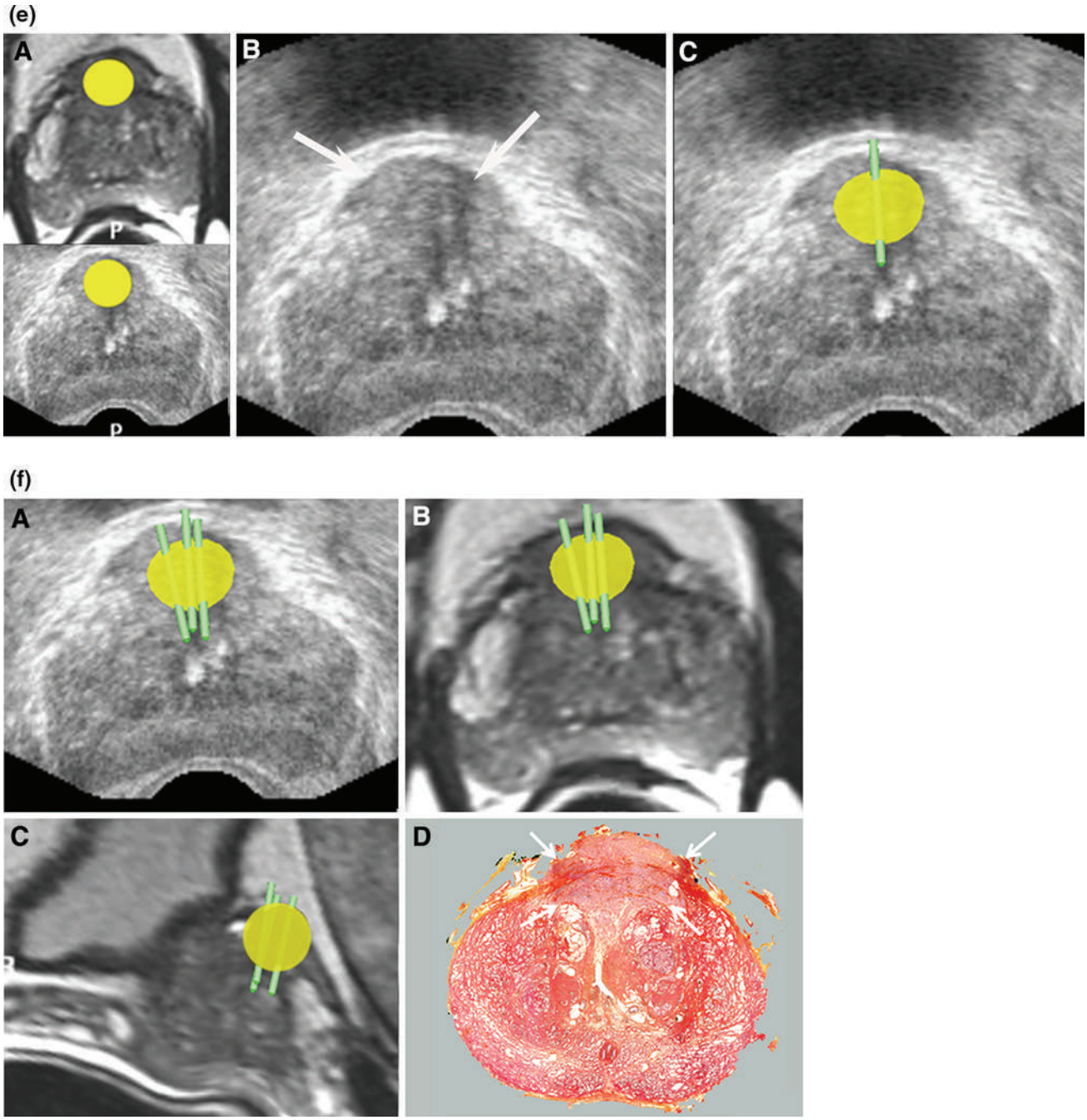


Fig. 9. continued

– In the study by Delongchamps et al. [19], comparing different registration techniques, the positive biopsy rate of significant cancers by deformable registration TB was significantly higher than those of SB and cognitive TB, but not higher than that of sensor registration TB (ESAOTE, Italy). However, the number of taken cores to reach this comparable result was significantly lower with the deformable system (3 vs 4).

– Baco and co-workers [33], in a series of 90 patients prior to initial biopsy with suspicion of prostate cancer, reported a 97% biopsy success rate within the target. Biopsy was positive in 52% of cases and the positive biopsy rate was strongly correlated to the MRI presumption of malignancy (91%, 27%, and 10% in targets with a high, intermediate, and low risk of malignancy, respectively). SB were negative in all patients with a negative MRI.

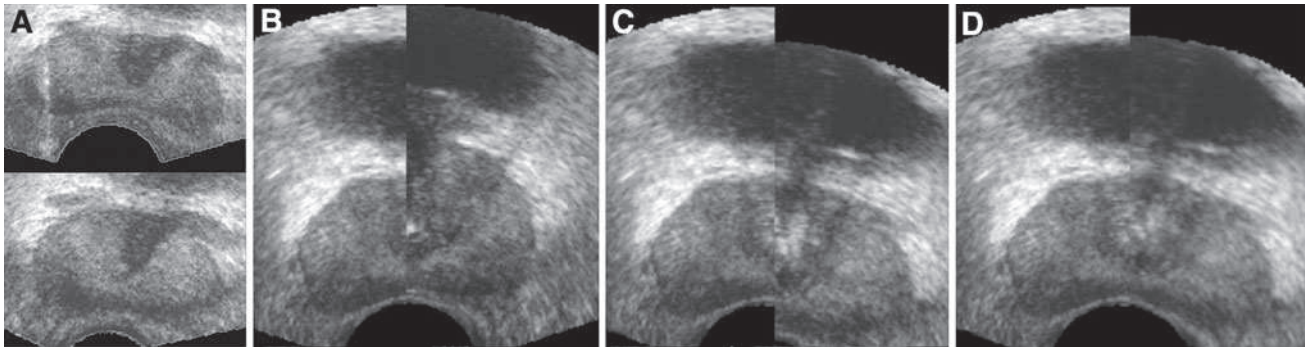


Fig. 10. TRUS–TRUS voxel-base registration. **A** Acquired image (*upper image*, during biopsy) and reference image (acquired during geometric elastic registration). **B** First step after determination of the plausible position of the prostate volume showing a poor registration. **C** Second step obtained with rigid registration refining the first estimation. **D** Elastic registration allowing for an accurate registration of the two images.

## Rationale for a TRUS–MRI image registration-based biopsy policy

TRUS–MRI image fusion is a technological advance which requires a reevaluation of the use of MRI in prostate cancer management, not only in patients with a diagnosed PCa but also for men before prostate biopsy. Multiparametric MRI is an established accurate technique to localize prostate cancer and may be thus used as a test to detect significant tumors. This concept is gaining more and more widespread acceptance, as there is growing evidence that random biopsies in areas without MRI abnormality show no cancer or insignificant tumors [19, 32–34]. Nevertheless, there are still challenging issues with regards to the potential role of MRI before biopsy.

- The first is currently gaining more and more widespread clinical acceptance: MRI should be recommended before a second set of biopsies in patients with a persistent biological suspicion of prostate cancer. TB should be performed to avoid to sample the prostate in the same areas as during the initial biopsy and to undersample unreachable areas (extreme apex and base and anterior portion of the prostate). Currently, a repeat second negative biopsy is falsely reassuring and the fear to miss a significant tumor generated the practice of template biopsy scheme (one transperineal biopsy every 5 $mm^2$ using a brachytherapy grid). This prostate mapping under general anesthesia improves, on computed models, the performance of repeat SB to detect tumors $>$0.2–0.5 cc [3], but may have a more limited value in vivo, because the prostate is a mobile organ whose shape and overlay to a metal grid change in real time with US probe and respiratory movements. Mismatch between the targeted area on the grid and the needle path can thus occur, as it has been shown in patients treated by brachytherapy [35]. Moreover, template prostate mapping is a complex procedure which entails a higher complication rate than SB, in particular a urinary retention rate of approximately 10% [36]. As a result, the accuracy of template prostate mapping in patients undergoing repeat biopsies needs further validation. Of note is the fact that the same conclusion may be drawn in patients under active surveillance which should benefit of MRI to decide if repeat biopsy should be performed. In this setting, a study has shown that the negative predictive value of MRI for excluding significant cancer, defined by the presence of Grade 4 on any core and a cancer length $>$4 mm was 90% [37].
- The second challenge is whether the MRI should be considered a triage test before initial biopsy to select patients requiring immediate TB in case of a positive MRI, while biopsy could be deferred if MRI shows no suspicious area [15, 34]. This strategy relies on the finding that PCa metastases within the same patient originated from a single precursor tumor focus [34]. This generated the concept of the dominant (or index) tumor which would be, despite the well-established multifocality of PCa [36], the only tumor focus to clone and lead to extraprostatic spread and metastases, would it be left untreated. Indolent secondary tumor foci (tumor volume $<$ 0.2–0.5 cc with no Gleason 4–5 grade) are not prone to progression and it had been shown years ago that these secondary indolent foci had no relationship with PSA biochemical failure in men undergoing radical retropubic prostatectomy [38]. When these secondary tumor foci are inapparent on MRI, 98% them are nonsignificant [39]. To detect the dominant tumor, the organ should thus be imaged with multiparametric MRI and the accuracy of TRUS–MRI image registration should be utilized to target suspicious areas, like for other organs of the body. In this strategy, SB would be obviated [15, 34].
- The third challenge is thus how to define a target on mp-MRI. Different scoring systems are currently used [12, 37, 40, 41], all including an individual three- or five-point scale T2/DW/DCE score and an overall

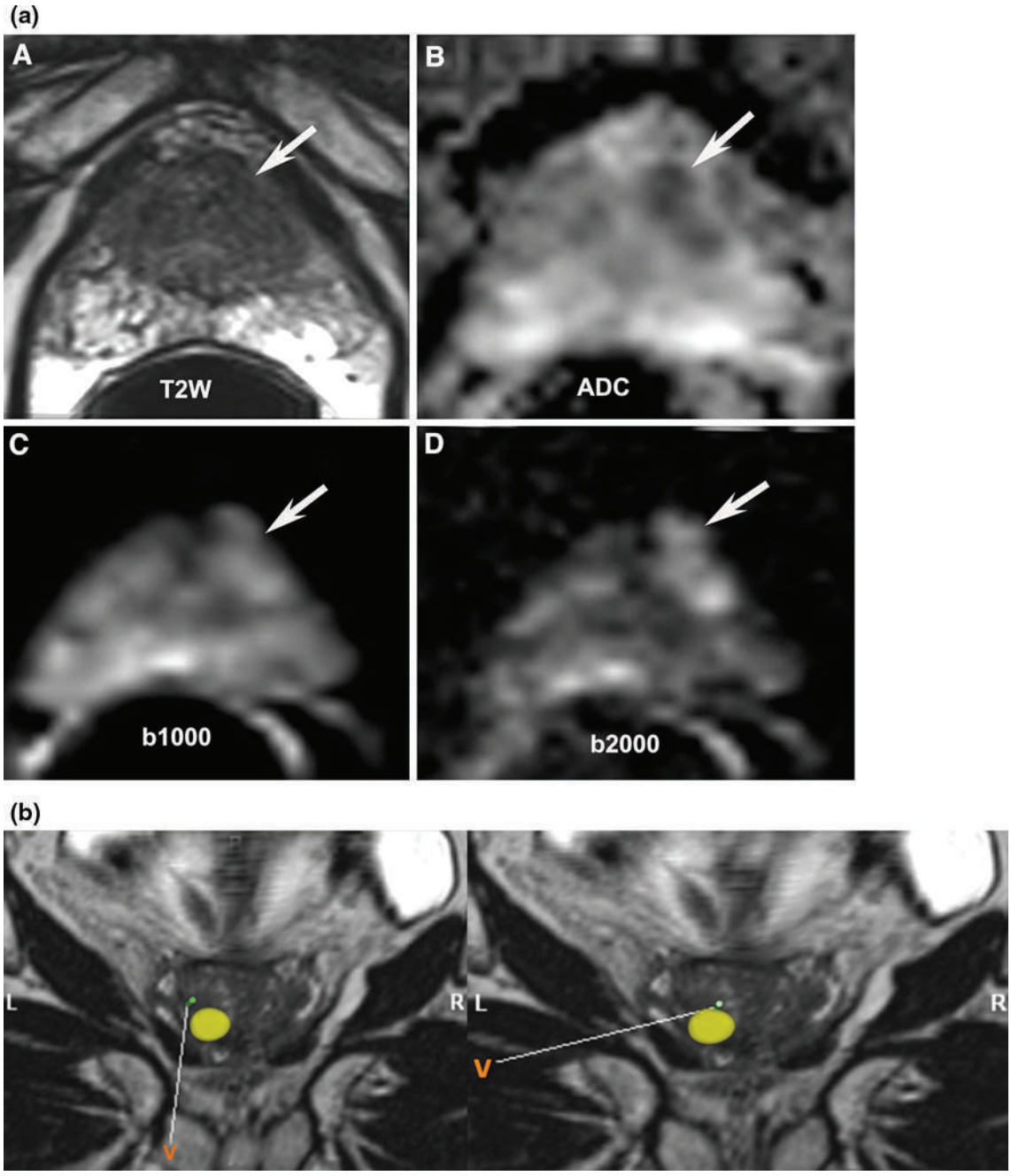


**Fig. 11.** Elastic registration with virtual biopsies. **a** Low signal intensity area, barely visible on T2W-MRI (*arrow*, **A**), with a low ADC value (*arrow*, **B**) and high intensity signal on DW source images, visible on b-1000 image (*arrow*, **C**), but much more conspicuous on b2000 image (*arrow*, **D**). **b** Two virtual biopsies (V) showing that the needle tract does not traverse the target. **c** After adjustment, three cores were taken from the lesion. The needle tracts (*green tags*) are visible within the target (*yellow tag*) on coronal and sagittal views of T2W (**A**, **B**) and DW-MRI (**C**, **D**). Gleason score 6 TZ cancer. Cancer length: 9 mm on two of the three cores.

five-point scale Likert score with a trend to take into account the dominant sequence according to the zone of origin of the lesion (DWI-MRI for the PZ and T2W-MRI for the TZ). ESUR guidelines have been published for scoring MRI focal abnormalities according to their presumption of malignity and are under evaluation [41]. Crucially, a standardized report is required to define what is benign or probably benign (score 1–2), equivocal (score 3), and probably malignant or malignant (scores 4–5). Follow-up of PSA level would be performed in patients with scores 1–2, because MRI can eliminate with a high accuracy the presence of significant cancer [19, 32, 37, 39] and would be thus a very effective tool to avoid over-

diagnosis of prostate cancer. Repeat or initial TB would be performed for scores 4–5. In the equivocal group (score 3), PSA surveillance combined with repeat MRI to update scoring or standard biopsies could be recommended. Because the degree of suspicion on MRI is a powerful predictor of significant cancer [25, 26, 32, 42], establishment of a standardized report becomes highly desirable.

- The fourth challenge is related to the growing evidence that DW-MRI plays a role in the evaluation of prognosis of PCa. High risk tumors (Gleason score $\geq 7_{4+3}$) have a significantly lower mean ADC value than that of the lower risk tumors. TRUS–MRI image fusion is an ideal tool to target foci with the highest impeded diffusion (which may contain high grade foci) by propagating the T2W-MRI target area to the DW-MRI (ADC or source images). This targeted strategy has been evaluated in a single study using cognitive registration, under MRI guidance, between T2W and DW-MRI which showed a concordance of biopsy and surgical Gleason score in 84% cases [43].
- The fifth and last challenge concerns the precision that should achieve image registration to provide the highest yield for prostate biopsies and its implication in focal therapy.
  - A study [44] evaluating the required accuracy for registration tools in the specific setting of targeting high grade cancer components within the tumor may provide the answer. The study showed that a spatial alignment of 1.9 mm was necessary for correct grading 95% of tumors. This targeting error is within the range of that observed with TRUS–MRI image registration systems. Organ-based registration may, however, be preferred to sensor-based registration as the former has the advantage of being robust with respect to patient movements. With this system, only image information is used to determine the position of the prostate to overlay the acquired and the reference volumes during registration. Moreover, sensor-based registration does not seem to provide the possibility of estimating organ deformation, as it would theoretically require to place a large number of sensors directly onto the organ. Because organ-based registration applies an organ deformation in both the planning and the guiding phase of the biopsy, this technology represents currently the state of the art of TRUS–MRI image registration, at the expense of a computational time which requires, during the guiding phase of the biopsy, a few seconds to have the registered images on screen instead of real-time control.
  - Implications for focal therapy can also be drawn from these evaluations. Currently, the transperineal approach is the reference standard and all the commercially available TRUS–MRI image registration systems have been developed for the transrectal route. However, the transrectal approach may not be contra-indicated for focal ablation and could be thus used more frequently in the future, would the concept of true focal ablation, aiming the tumor focus and not the moiety of the prostate, be validated.

## References


1. Schroder FH, Hugosson J, Roobol MJ, et al. (2009) Screening and prostate-cancer mortality in a randomized European study. N Engl J Med 360(13):1320–1328
2. Suardi N, Capitanio U, Chun FK, et al. (2008) Currently used criteria for active surveillance in men with low-risk prostate cancer: an analysis of pathologic features. Cancer 113(8):2068–2072
3. Hu Y, Ahmed HU, Carter T, et al. (2012) A biopsy simulation study to assess the accuracy of several transrectal ultrasonography (TRUS)-biopsy strategies compared with template prostate mapping biopsies in patients who have undergone radical prostatectomy. BJU Int 110:812–820
4. Nam RK, Saskin R, Lee Y, et al. (2010) Increasing hospital admission rates for urological complications after transrectal ultrasound guided prostate biopsy. J Urol 183(3):963–968
5. Pelzer A, Bektic J, Berger AP, et al. (2005) Prostate cancer detection in men with prostate specific antigen 4 to 10 ng/ml using a combined approach of contrast enhanced color Doppler targeted and systematic biopsy. J Urol 173(6):1926–1929
6. Aigner F, Pallwein L, Schocke M, et al. (2011) Comparison of real-time sonoelastography with T2-weighted endorectal magnetic resonance imaging for prostate cancer detection. J Ultrasound Med 30(5):643–649
7. Simmons LA, Autier P, Zat'ura F, et al. (2012) Detection, localisation and characterisation of prostate cancer by prostate HistoScanning(TM). BJU Int 110(1):28–35
8. Koh DM, Collins DJ (2007) Diffusion-weighted MRI in the body: applications and challenges in oncology. AJR Am J Roentgenol 188(6):1622–1635
9. Franiel T, Hamm B, Hricak H (2011) Dynamic contrast-enhanced magnetic resonance imaging and pharmacokinetic models in prostate cancer. Eur Radiol 21(3):616–626
10. Hoeks CM, Barentsz JO, Hambrock T, et al. (2011) Prostate cancer: multiparametric MR imaging for detection, localization, and staging. Radiology 261(1):46–66
11. Vourganti S, Rastinehad A, Yerram NK, et al. (2012) Multiparametric magnetic resonance imaging and ultrasound fusion biopsy detect prostate cancer in patients with prior negative transrectal ultrasound biopsies. J Urol 188:2152–2157
12. Natarajan S, Marks LS, Margolis DJ, et al. (2011) Clinical application of a 3D ultrasound-guided prostate biopsy system. Urol Oncol 29(3):334–342
13. Moore CM, Robertson NL, Arsanious N, et al. (2013) Image-guided prostate biopsy using magnetic resonance imaging-derived targets: a systematic review. Eur Urol 63:125–140
14. Lawrentschuk N, Haider MA, Daljeet N, et al. (2010) 'Prostatic evasive anterior tumours': the role of magnetic resonance imaging. BJU Int 105(9):1231–1236
15. Haffner J, Lemaitre L, Puech P, et al. (2011) Role of magnetic resonance imaging before initial biopsy: comparison of magnetic resonance imaging-targeted and systematic biopsy for significant prostate cancer detection. BJU Int 108:E171–E178
16. Labanaris AP, Zugor V, Smiszek R, et al. (2010) Guided e-MRI prostate biopsy can solve the discordance between Gleason score biopsy and radical prostatectomy pathology. Magn Reson Imaging 28(7):943–946
17. Kvale R, Moller B, Wahlqvist R, et al. (2009) Concordance between Gleason scores of needle biopsies and radical prostatectomy specimens: a population-based study. BJU Int 103(12):1647–1654
18. Lattouf JB, Grubb RL 3rd, Lee SJ, et al. (2007) Magnetic resonance imaging-directed transrectal ultrasonography-guided biopsies in patients at risk of prostate cancer. BJU Int 99(5):1041–1046
19. Delongchamps NB, Peyromaure M, Schull A, et al. (2013) Prebiopsy magnetic resonance imaging and prostate cancer detection:

comparison of random and targeted biopsies. J Urol 189(2):493–499
20. Puech P, Rouviere O, Renard-Penna R, et al. (2013) Prostate cancer diagnosis: multiparametric MR-targeted biopsy with cognitive and transrectal US-MR fusion guidance versus systematic biopsy—prospective multicenter study. Radiology. doi:10.1148/radiol.13121501
21. Ukimura O, Faber K, Gill IS (2012) Intraprostatic targeting. Curr Opin Urol 22(2):97–103
22. Baumann M, Mozer P, Daanen V, Troccaz J (2012) Prostate biopsy tracking with deformation estimation. Med Image Anal 16(3):562–576
23. Mouraviev V, Pugnale M, Kalyanaraman B, et al. (2013) The feasibility of multiparametric magnetic resonance imaging for targeted biopsy using novel navigation systems to detect early stage of prostate cancer: the preliminary experience. J Endourol 27(7):820–825
24. Bax J, Cool D, Gardi L, et al. (2008) Mechanically assisted 3D ultrasound guided prostate biopsy system. Med Phys 35(12):5397–5410
25. Sonn GA, Natarajan S, Margolis DJ, et al. (2013) Targeted biopsy in the detection of prostate cancer using an office based magnetic resonance ultrasound fusion device. J Urol 189(1):86–91
26. Sonn GA, Chang E, Natarajan S, et al. (2013) Value of targeted prostate biopsy using magnetic resonance-ultrasound fusion in men with prior negative biopsy and elevated prostate-specific antigen. Eur Urol. doi:10.1016/j.eururo.2013.03.025
27. Singh AK, Kruecker J, Xu S, et al. (2008) Initial clinical experience with real-time transrectal ultrasonography-magnetic resonance imaging fusion-guided prostate biopsy. BJU Int 101(7):841–845
28. Xu S, Kruecker J, Turkbey B, et al. (2008) Real-time MRI-TRUS fusion for guidance of targeted prostate biopsies. Comput Aided Surg 13(5):255–264
29. Pinto PA, Chung PH, Rastinehad AR, et al. (2011) Magnetic resonance imaging/ultrasound fusion guided prostate biopsy improves cancer detection following transrectal ultrasound biopsy and correlates with multiparametric magnetic resonance imaging. J Urol 186(4):1281–1285
30. Martin S, Troccaz J, Daanen V (2010) Automated segmentation of the prostate in 3D MR images using a probabilistic atlas and a spatially constrained deformable model. Med Phys 37(4):1579–1590
31. Ukimura O, Desai MM, Palmer S, et al. (2012) 3-Dimensional elastic registration system of prostate biopsy location by real-time 3-dimensional transrectal ultrasound guidance with magnetic resonance/transrectal ultrasound image fusion. J Urol 187(3):1080–1086
32. Portalez D, Mozer P, Cornud F, et al. (2012) Validation of the European Society of urogenital radiology scoring system for prostate cancer diagnosis on multiparametric magnetic resonance imaging in a cohort of repeat biopsy patients. Eur Urol 62:986–996
33. Rud E, Baco E, Eggesbo HB (2012) MRI and ultrasound-guided prostate biopsy using soft image fusion. Anticancer Res 32:3–9
34. Ahmed HU, Kirkham A, Arya M, et al. (2009) Is it time to consider a role for MRI before prostate biopsy? Nat Rev Clin Oncol 6(4):197–206
35. Lagerburg V, Moerland MA, Lagendijk JJ, Battermann JJ (2005) Measurement of prostate rotation during insertion of needles for brachytherapy. Radiother Oncol 77(3):318–323
36. Sartor AO, Hricak H, Wheeler TM, et al. (2008) Evaluating localized prostate cancer and identifying candidates for focal therapy. Urology 72(6 Suppl):S12–S24
37. Arumainayagam N, Ahmed HU, Moore CM, et al. (2013) Multiparametric MR imaging for detection of clinically significant prostate cancer: a validation cohort study with transperineal template prostate mapping as the reference standard. Radiology. doi:10.1148/radiol.13120641
38. Stamey TA, McNeal JM, Wise AM, Clayton JL (2001) Secondary cancers in the prostate do not determine PSA biochemical failure in untreated men undergoing radical retropubic prostatectomy. Eur Urol 39(Suppl 4):22–23
39. Moore CM, Robertson NL, Arsanious N, et al. (2013) Image-guided prostate biopsy using magnetic resonance imaging-derived targets: a systematic review. Eur Urol 63(1):125–140
40. Delongchamps NB, Rouanne M, Flam T, et al. (2011) Multiparametric magnetic resonance imaging for the detection and localization of prostate cancer: combination of T2-weighted, dynamic contrast-enhanced and diffusion-weighted imaging. BJU Int 107(9):1411–1418
41. Barentsz JO, Richenberg J, Clements R, et al. (2012) ESUR prostate MR guidelines 2012. Eur Radiol 22(4):746–757
42. Rud E, Baco E, Eggesbo HB (2012) MRI and ultrasound-guided prostate biopsy using soft image fusion. Anticancer Res 32(8):3383–3389
43. Hambrock T, Hoeks C, Hulsbergen-van de Kaa C, et al. (2012) Prospective assessment of prostate cancer aggressiveness using 3-T diffusion-weighted magnetic resonance imaging-guided biopsies versus a systematic 10-core transrectal ultrasound prostate biopsy cohort. Eur Urol 61(1):177–184
44. van de Ven WJ, Hulsbergen-van de Kaa CA, Hambrock T, Barentsz JO, Huisman HJ (2012) Simulated required accuracy of image registration tools for targeting high-grade cancer components with prostate biopsies. Eur Radiol 23:1401–1407